

AIAS 2019 International Conference on Stress Analysis

# Experimental evaluation of artificial defects using SMArt thermography

De Giorgi Marta<sup>a</sup>, Nobile Riccardo<sup>a\*</sup>, Saponaro Andrea<sup>a</sup>

<sup>a</sup>*Department of Engineering for Innovation, University of Salento, Via Arnesano, 73100 Lecce, Italy*

## Abstract

SMArt thermography is an innovative and promising technique that could be useful for the detection of damages of large components subjected to in-service loads, like wind blade. This technique requires building traditional carbon or glass fiber reinforced composite laminates adding a regular net of Shape Memory Alloy (SMA) wires in the matrix. These wires confer to the composite material additional features. In particular, the electro-thermal properties of SMA could be used as an internal heat source to be used for the control of the component using the traditional numerical technique used to elaborate the raw thermal data. Despite of other thermography techniques, SMArt thermography is characterized by a quite reduced amount of heating power, which produces a limited increasing of the temperature of the component subjected to control. On the other hand, the numerical elaboration of thermal data acquired from IR camera is more sensitive and require a deeper comprehension of the phenomena. In this work, a GFRP composite panel containing several artificial defects has been studied both from a numerical and experimental point of view, in order to determine the sensitivity of the technique, the limit of applicability and practical indications about the reliability of the technique.

© 2019 The Authors. Published by Elsevier B.V.

This is an open access article under the CC BY-NC-ND license (<http://creativecommons.org/licenses/by-nc-nd/4.0/>)

Peer-review under responsibility of the AIAS2019 organizers

*Keywords:* Shape Memory Alloy; multifunctional materials; SMArt thermography;

## 1. Introduction

Composite materials are conceived to obtain mechanical properties that are optimized for the stress state they are subjected, allowing to obtain the best configuration for a given component. This peculiarity and the relatively facility

---

\* Corresponding author. Tel.: +39-832-297771; fax: +39-832-297768.  
E-mail address: [riccardo.nobile@unisalento.it](mailto:riccardo.nobile@unisalento.it)

## Nomenclature

$C_a$	absolute thermal contrast
$C_n$	normalized thermal contrast
DID	Defect Index Dimension
$d$	defect diameter
$h$	defect depth
SMA	Shape Memory Alloy
$T_d$	temperature of defect zone
$T_i$	temperature of integer zone
$t_0$	time at the end of the heating phase

to realize and assembly large structural components justify the extensive use that composite materials experiments in the last years in an increasing number of applications. However, even if the main function of a structural component is to sustain the applied load in the predicted environmental condition, it is possible that other secondary functions are required, which could depend by its specific ambit of use. From this point of view, composite material offers several advantages with respect to traditional homogeneous materials, since it is possible to enhance the material properties simply introducing other additional components to the fundamental ones fiber and matrix. Additives could be added to matrix or lodged on the fiber to obtain specific behavior or to increase inherent properties; alternatively, fiber of different nature could be added to the matrix. The resulting material continues to be defined as a composite material from a structural point of view, but due to its capacity to absolve to several functions a definition of multifunctional material is more appropriate. How it is possible to imagine, the variety of multifunctional materials that have been proposed is very vast and not exhaustive at all. Among them, a particular category is obtained if metallic wires are embedded in the composite. The hybrid metal/carbon fiber or metal/glass fiber composite is generally characterized by high mechanical properties and improved impact strength. Additionally, they can enhance the possibility to detect inherent or load induced damage, or allowing the strain sensing, or finally act as thermal heat sources for de-icing for aeronautical purposes (Rizzo et al, 2019).

The particular multifunctional material that has been considered in this work is realized embedding Shape Memory Alloy (SMA) wires in traditional carbon or glass fiber reinforced composite laminates known as SMART composites. The introduction of SMA wires in a composite act as a secondary reinforcement for the composite, giving in particular an increase of the impact resistance of material, thanks to the possibility of dissipating energy during the martensitic phase transformation that this kind of material suffer when subjected to plastic deformations. Moreover, a grid of SMA wires inserted in the composite, if an opportune electrical current is applied, is capable to constitute an internal heat source that simplify the application of non-destructive technique based on thermography. Such a system enables a built-in, fast, cost-effective and in-depth assessment of the structural damage as it overcomes the limitations of standard thermography.

Technical literature about composite material enhanced with the insertion of SMA wires is relatively limited. A resume of the mechanical properties improvements that can be obtained is reported by Angioni et al. (2011). Other applications consist in the use of SMA wires as strain sensing integrated in the composite, with the main aim of evaluating the damage progress due to impact or load application, rather than the reliable evaluation of the stress state (Nagai and Oishi (2006), Oishi and Nagai (2005), Cui et al. (2010)).

A fundamental effort for this kind of material is represented by the non-destructive control, which will assure the absence of potentially dangerous defects. In industrial applications, the standard control is represented by ultrasonic measurement, but the possibility to use reliable thermographic techniques constitutes an important challenge, due to the possibility of simplifying the control and reducing the cost. A relevant literature exists about thermographic technique for control purposes, starting from the fundamental work of Maldague (2002). However, the first idea to introduce a heat source layer embedded in a composite laminate for non-destructive control purposes was successfully exploited by Ahmed et al., (2008), even if the solution was excessively invasive with respect to the mechanical behavior of the material. Also the insertion of 3D electrical circuit in the composite (Orłowska et al. (2011)) could potentially lead to a worsening of the mechanical properties of the material, which is unacceptable for

several applications. A simpler and less invasive solution has been proposed by Pinto et al. (2014) and successively by Angioni et al. (2016). In this case a simple grid of SMA wires is inserted between two plies and the influence of various parameters on the detecting possibility has been considered. The comparison of the traditional active thermography with the respect to the introduction of diffused internal heat sources is graphically represented in Figure 1.

This solution was adopted in a preliminary work of the authors (De Giorgi et al. (2018)). In this work, a numerical study has been carried out to evaluate the thermal output of a GFRP laminate with embedded SMA wires, with the aim of determining the optimal parameters that could allow the use of this material in active infrared thermography. In the same work the numerical simulation has been experimentally verified, observing how it is possible to obtain a quite uniform initial heating of the component and to simplify significantly the traditional set-up of thermographic control. However, the practical application of SMARt thermography to the control of industrial components presupposes the determination of the applicability limit and the reliability of the technique. The first step is therefore to introduce in a representative component known artificial defects having different dimensions and localizations and try to individuate it. This is the objective that has been pursued in this work.

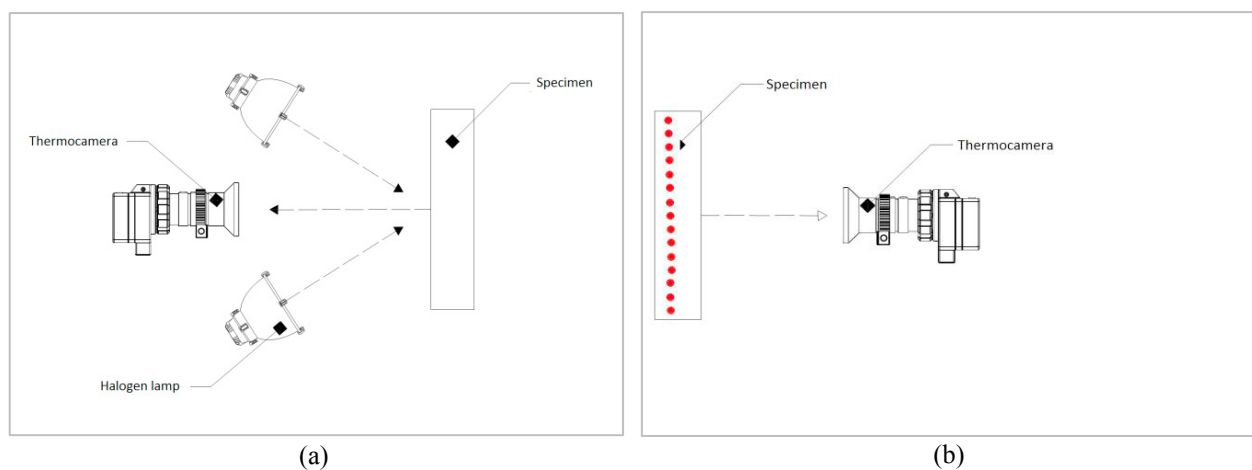


Fig. 1. Schematics of traditional active thermography (a) and material enabled thermography (b).

## 2. Materials and methods

A flat GFRP laminate panel constituted by 8 unidirectional plies has been considered in this study. The panel has dimension of 210 x 300 mm, an overall thickness of about 8 mm and is constituted by 8 plies having a common orientation of  $0^\circ$ . This particular stacking sequence has been considered, since it is the most common used for the realization of the high stressed zones of wind blades, which is the industrial component selected for this application. The panel contains two grids of SMA wires made of Flexinol® having a diameter of 0.25 mm: the horizontal one is localized in the middle thickness of the panel, between 4<sup>th</sup> and 5<sup>th</sup> plies, while the vertical grid is inserted between 2<sup>nd</sup> and 3<sup>rd</sup> plies. An array of 16 defects is inserted at various locations inside the panel. One of this is constituted by a clearance hole. All the defects are approximatively located in the middle of the grid of SMA wires, which is the worst condition for the determination of the presence of the defect (Pinto et al. (2014)). The geometry of the panel and the localization of the defects are reported in Figure 2, while Table 1 resumed the main geometrical parameters of each defect. The thermal map caused by the Joule effect was monitored using the infrared thermocamera FLIR 7550, having a thermal resolution of 20 mK.

The thermal behaviour of a similar panel without defects was numerically and experimentally studied in a previous work (De Giorgi et al., (2018)). In that work, authors showed that is possible to obtain a temperature increase of about 1.5 K applying a direct current of 16.5 V for a time of 120 s and corresponding to a power source of  $7 \times 10^6 \text{ W/m}^3$ .

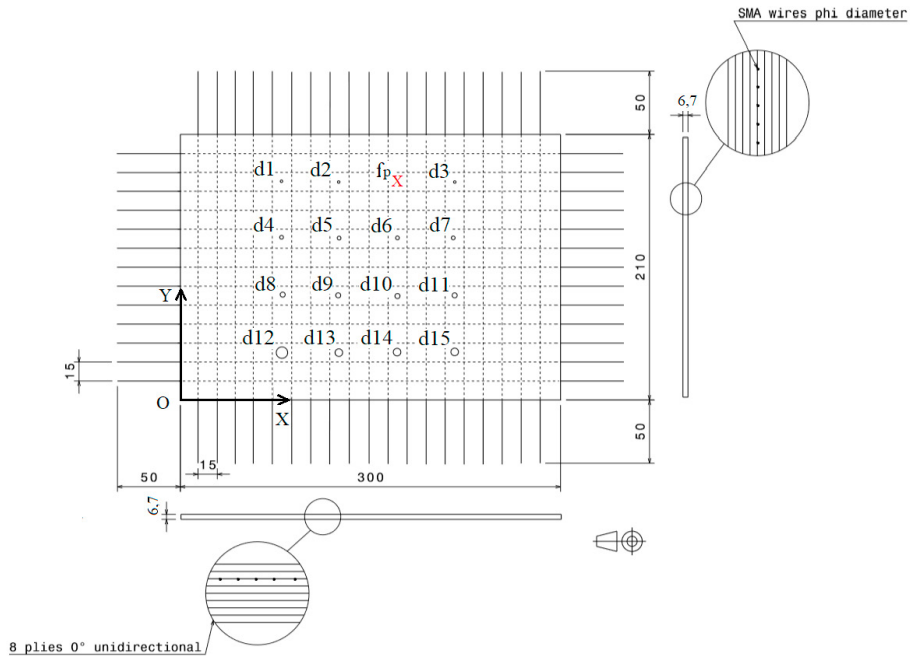


Fig. 2. Geometry of the panel with indication of the SMA wire grids and defect localization

Table 1. Detail of defects introduced in the panel

Defect	Diameter d [mm]	Depth h [mm]
d1	2	1
d2	2	2.6
d3	2	1.8
d4	3	1
d5	3	2
d6	3	3
d7	3	2.5
d8	4	1
d9	4	2
d10	4	2.6
d11	4	4
d12	9	2.7
d13	6	4
d14	6	5.35
d15	6	4
fp	2	clearance hole

### 3. Experimental results and discussion

A Pulsed Thermography technique was used for the experimental evaluation of the defects. The elaboration of the raw data has been carried out using a routine Matlab that allow calculating the absolute contrast and the relative

contrast, defined as follows:

$$C_a(t) = T_d(t) - T_i(t) \quad (1)$$

$$C_n(t) = \left( \frac{T_d(t)}{T_d(t_0 + 1)} \right) - \left( \frac{T_i(t)}{T_i(t_0 + 1)} \right) \quad (2)$$

with the following significance of the parameters:

- $T_d(t)$  and  $T_d(t_0+1)$  temperature of the defect zone respectively at time  $t$  and immediately after the end of the heating phase ( $t_0+1$ )
- $T_i(t)$  and  $T_i(t_0+1)$  temperature of the integer zone respectively at time  $t$  and immediately after the end of the heating phase ( $t_0+1$ )

In order to establish the better parameters for the defect evaluations, different duration of heating time and heat power was applied. The first result obtained was foreseeable and observed by other authors (Pinto et al. (2014)): the possibility of defect detection is assured only if the defect is between the SMA grid, which is the heat source, and the thermocamera. For this reason, since the large part of defects is located at a depth almost equal or higher than 4 mm, the only results that have been reported in this work are referred to the use of the vertical grid, which is located between 2<sup>nd</sup> and 3<sup>rd</sup> plies of the laminate. A power source of  $7 \times 10^6$  W/m<sup>3</sup> was used and the heating phase was varied between 120s and 600 s, followed by an acquisition of the subsequent cooling varying from 600 s to 1500 s. However, the best combination of parameters used for the defect evaluation consists in a heating phase having duration of 480 s and a subsequent acquisition of 1500 s. It is important to observe that the duration of each measurement is highly increased with respect to traditional PT technique, which could potentially represents a limitation due to the need of collecting a high amount of data during measurements.

Using these measurement conditions, the raw data corresponding to the thermal map about 150 s after the end of the heating phase allow determining the defects reported in Figure 3. Starting from these data, the spatial thermal profile along a line crossing defect d12 could be obtained (Fig. 4). The defect appears as a low temperature region, due to the reduction of the thermal conductivity introduced by the defect. The thermal difference between the defect region and the surrounding zone is relatively low, about 0.8 K, but clearly measurable.

An example of data elaboration is reported for defect d12. In detail, the elaboration procedure starts with the individuation of the defect zone and of the surrounding integer zone (Fig. 5a). In this choice, the operator is guided by the isothermal lines that are traced by the routine. Successively, the procedure allows calculating and plotting the trends of the mean temperature over time of the two zones (Fig. 5b), which clearly highlighted the presence of the

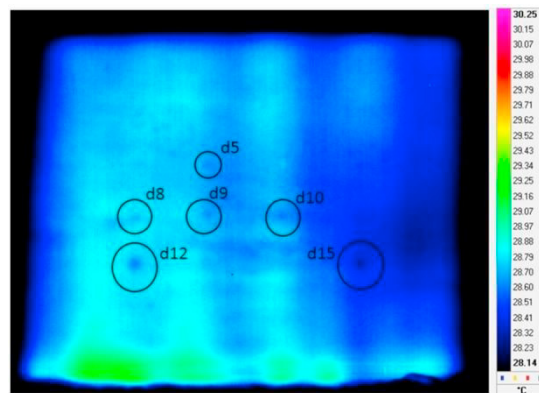


Fig. 3. Thermal map of the panel after about 150 s

defect. Finally, the plot of the absolute and normalized contrasts is obtained for a quantitative evaluation of the defect (Fig. 5c-d). Applying the same procedure to all the defect showed in Figure 3, it is possible to obtain the characteristics values of the contrast for each defect, which are reported in Table 2.

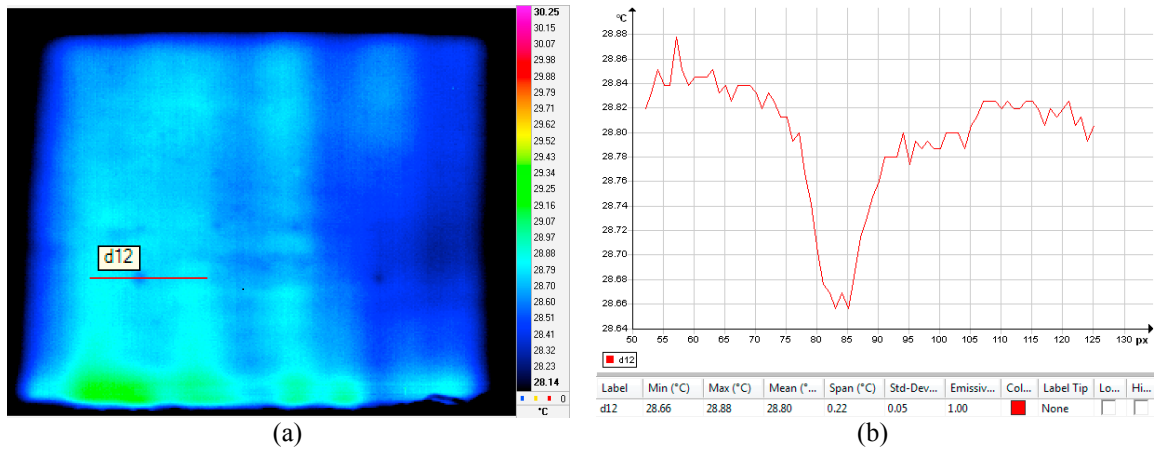


Fig. 4. a) Thermal map of the panel; b) spatial thermal profile of defect d12

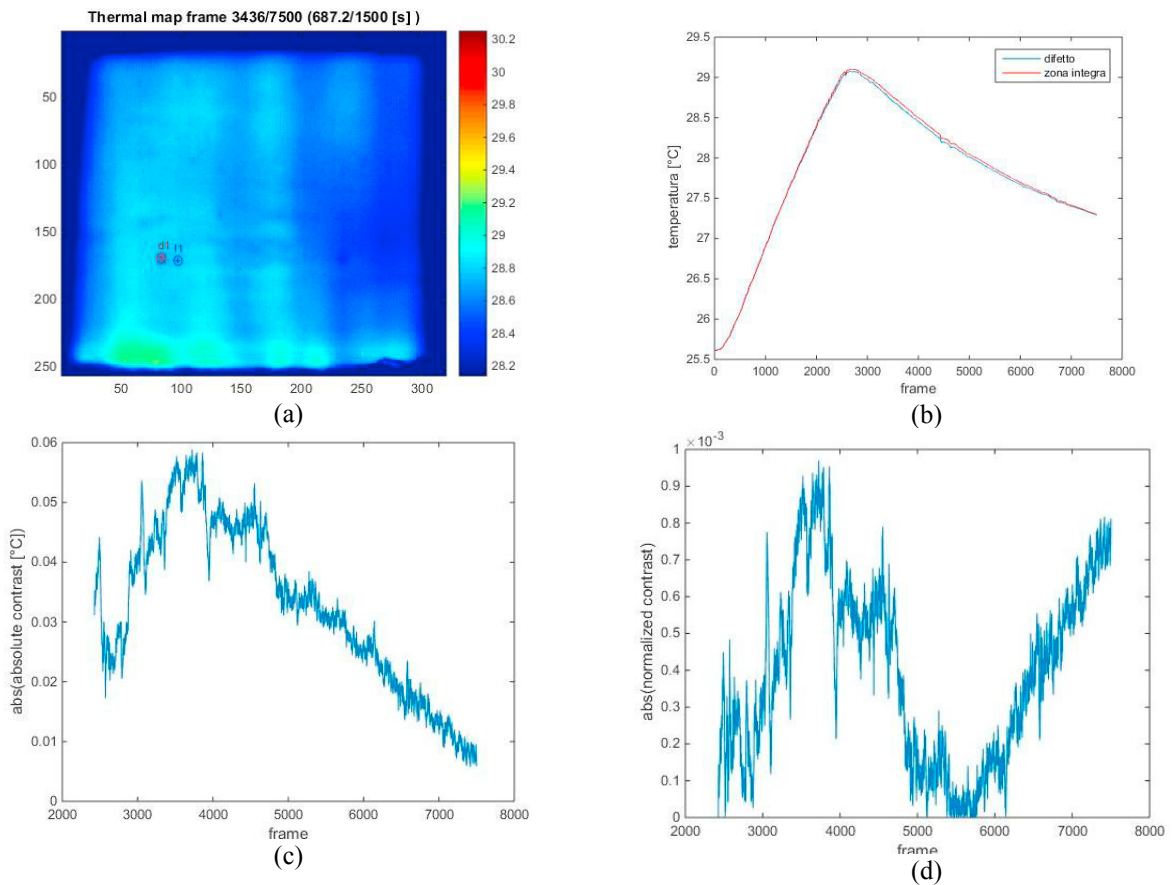


Fig. 5. Elaboration of thermal map: a) selection of defect and integer zone, b) thermal trend over time of the two zones, c) calculation of absolute contrast and d) of normalized contrast

Table 2. Thermal characterization of detected defects

Defect	Diameter d [mm]	Depth h [mm]	Absolute contrast $C_{a\_max}$ [K]	Normalized contrast $C_{n\_max}$
d5	3	2	0.0336	0.0013
d8	4	1	0.0399	8.63E-04
d9	4	2	0.0306	0.011
d10	4	2.6	0.0494	0.0012
d12	9	2.7	0.0588	0.0015
d13	6	4	0.0601	0.0016
d15	6	4	0.028	0.001

Observing the data reported in Table 2, it is possible to establish that the minimum dimension of the defect that could be detected is of 4 mm, with the exception of defect d5 that has a diameter of 3 mm. It is important to notice that the localization of defect was chosen to be exactly in the middle region between two subsequent wires, that is the worst condition for the defect detection. Therefore, the technique would be able potentially to detect defect with lower dimensions, if positioned close to the embedded wires. Another important point is that the depth of defect is not so important for its detectability. It is well known that a limitation of the thermographic technique is the possibility to individuate defect at limited depth within the material. This is due to the fact that the heating source is outside the material and a thermal gradient between surface and the inner material is obtained using external heat sources. This circumstance is on the other hand absent in SMART thermography. It is only required that the defect is between SMA wires and external surface, suggesting the convenience of inserting SMA wires at the lowest depth.

In order to obtain quantitative data on the detection capabilities of the technique, it is possible to introduce a normalized parameter that has been called Defect Index Dimension (DID), which identifies each defect with the following definition:

$$DID = d_i * \frac{h_i}{t} \quad (3)$$

in which:

$d_i$  is the diameter of the defect

$h_i$  is the depth of the defect

$t$  is the plate thickness.

Using this parameter, a quite linear correlation between absolute contrast  $C_a$  and DID could be obtained, with the exception of datum of d15 defect, which is however characterized by a value of the absolute contrast unusually low (Fig. 6).

A better visualization and identification of defect distribution might be obtained using an algorithm for the elaboration of the map temperature called Local Boundary Contrast (LBC), which has been recently proposed (Dattoma et al. ref. 1 (2018), Dattoma et al. ref. 2 (2018)). This procedure overcomes the need to individuate the defect and integer zones, choice which is subjected to the personal evaluation of the operator. The algorithm is based on the definition of a correlation window having a fixed extension around each pixel. For each pixel a local contrast is calculated as the difference of the central pixel with the mean temperature of the surrounding pixels of the correlation window. The local contrast that has been calculated could be used to rebuild the map of the panel using a grey-scale, which allowed an easy and reliable visualization of all the defects (Fig. 7). Another advantage of this technique is the simplification in the evaluation of defect dimension: defect d12 for example is estimated to have a diameter of 10 pixels, while distance between defects d12 and d15 is of 150 pixels. Since the absolute distance between these two defects is known and equal to 135 mm, it is possible to establish with a simple proportion a dimension of the defect of 9 mm, which correspond exactly to the effective dimension of the defect.

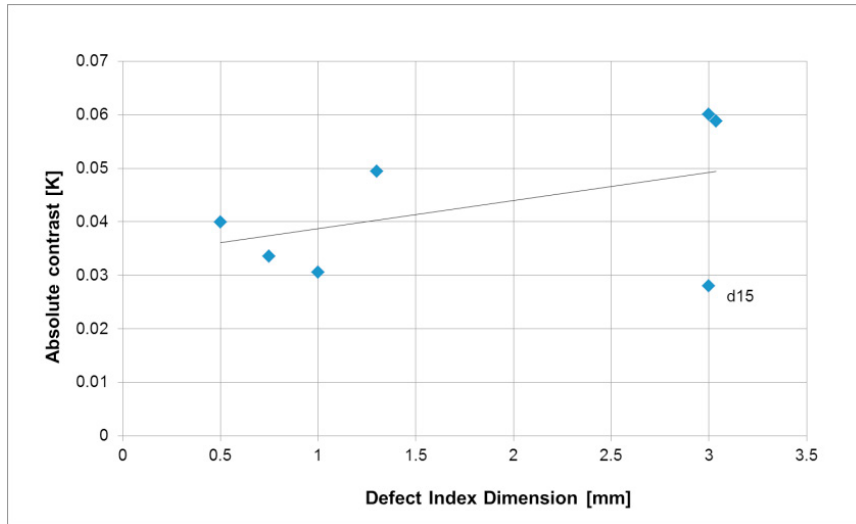


Fig. 6. Correlation between evaluated absolute contrast and Defect Index Dimension

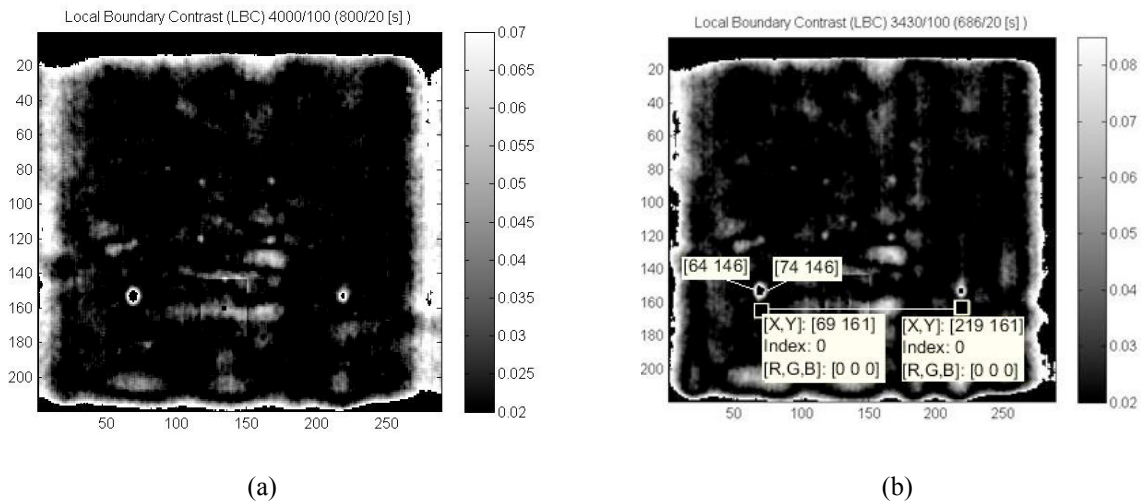


Fig. 7. Application of LBC algorithm: a) defect distribution on the panel, b) evaluation of defect d12 dimension

## Conclusion

The capability of SMARt thermography to individuate artificial defect inserted in a GFRP composite panel has been evaluated using a Pulsed Thermography approach. The experimental measurement showed the possibility to detect defect having a minimum diameter of 4 mm, without any particular limitation with respect to the depth of the defect. However, the detection is possible only if the defect is localized between SMA wires and inspected surface, suggesting the need to insert the SMA wires at the highest depth. On the other hand, the technique requires using high heating time and subsequent cooling time for an efficient defect detection, which could constitute a limitation for the large amount of collected data.

A quantitative evaluation of the relation between the absolute contrast and the parameter Defect Index Dimension, which identified the combination of diameter and depth of the defect, has been found, while the use of the LBC technique allowed a better visualization and evaluation of the defect dimensions.



## Acknowledgements

This work has been financially supported by the project PRIN 2015 “Smart Optimized Fault Tolerant WIND turbines” – SOFTWIND funded by Italian Ministry of University and Research.

## References

- Ahmed, T., Nino, G., Bersee, H., Beukers, A., 2008. Heat emitting layers for enhancing NDE of composite structures, *Composites A Appl. Sci. Manuf.*, 39, 1025-1036
- Angioni, S.L., Ciampa, F., Pinto, F., Scarselli, G., Almond, D.P., Meo, M., 2016. An Analytical Model for Defect Depth Estimation Using Pulsed Thermography, *Experimental Mechanics*, 56, 6, 1111–1122.
- Angioni, S.L., Meo, M., Foreman, A., 2011. Impact damage resistance and damage suppression properties of shape memory alloys in hybrid composites—a review, *Smart Mater. Struct.* 20.
- Cui, D., Song, G., Li, H., 2010. Modeling of the electrical resistance of shape memory alloy wires, *Smart Mater Struct*;19(5).
- Dattoma, V., Nobile, R., Panella, F.W., Saponaro, A., 2018. NDT thermographic techniques on CFRP structural components for aeronautical applications, *Procedia Structural Integrity*, 8, 452-461.
- Dattoma, V., Nobile, R., Panella, F.W., Pirinu, A., Saponaro, A., 2018. Advanced NDT procedures and thermal data processing on CFRP aeronautical components, *Proceedings IRF2018 of 6<sup>th</sup> International Conference Integrity-Reliability-Failure* (ed. J.F. Siva Gomes and S.A. Meguid), Lisbon 22-26 July 2018.
- De Giorgi, M., Nobile, R., 2018. A possible use of SMARt thermography for the control of GFRP composite laminate, *Procedia Structural Integrity*, 12, 239-248.
- Maldague, X.P., 2002. Introduction to NDT by active infrared thermography, *Mater Eval*; 60(9):1060–73.
- Nagai, H., Oishi, R., 2006. Shape memory alloys as strain sensors in composites, *Smart Mater Struct*;15(2):493.
- Oishi, R., Nagai, H., 2005. Strain sensors of shape memory alloys using acoustic emissions, *Sensors Actuators A: Phys*;122(1):39–44.
- Orlowska, A., Kolakowski, P., Holnicki-Szulc, J., 2011. Detecting delamination zones in composites by embedded electrical grid and thermographic method, *Smart Mater. Struct.*, 20, 105009
- Pinto, F., Maroun, F.Y., Meo, M., 2014. Material enabled thermography, *NDT&E International* 67, 1–9.
- Rizzo, F., Pinto, F., Meo, M., 2019. Development of multifunctional hybrid metal/carbon composite structures, *Composite Structures*, 222: 110907.